Supplemental Figure. 1. Human TRMT1 and TRMT1L contain subcellular localization signals. (A) Prediction of bipartite nuclear localization signals in TRMT1 and TRMT1L using cNLS Mapper (http://nls-mapper.iab.keio.ac.jp/cgi-bin/NLS_Mapper_form.cgi). (B) Prediction of a mitochondrial targeting signal and cleavage sites in TRMT1 using (B) MitoFates (http://mitf.cbrc.jp/MitoFates/cgi-bin/top.cgi) or (C) TPpred2 (http://tppred2.biocomp.unibo.it/tppred2). Proteolytic cleavage sites in TRMT1 for mitochondria processing peptidase (MPP) and intermediate cleavage peptidase 55 (Icp55) were predicted using MitoFates. For TPpred2, two mitochondrial cleavage sites are predicted as defined: R3a = RX [FLY]j[SA] and R3b = RX[FLY]jX. (D) TRMT1 tagged with GFP was transiently expressed in HeLa cells with mitochondrial staining using Chromeo live cell stain and nuclear staining with DAPI.

Supplemental Figure 2. PHA assay on mitochondrial tRNAs. An increase in signal for the D-AC PHA probe was detected for mitochondrial tRNA-Ile-GAU isolated from TRMT1-KO cells. No change in PHA signal was detected for any of the other mitochondrial tRNAs containing G at position 26.

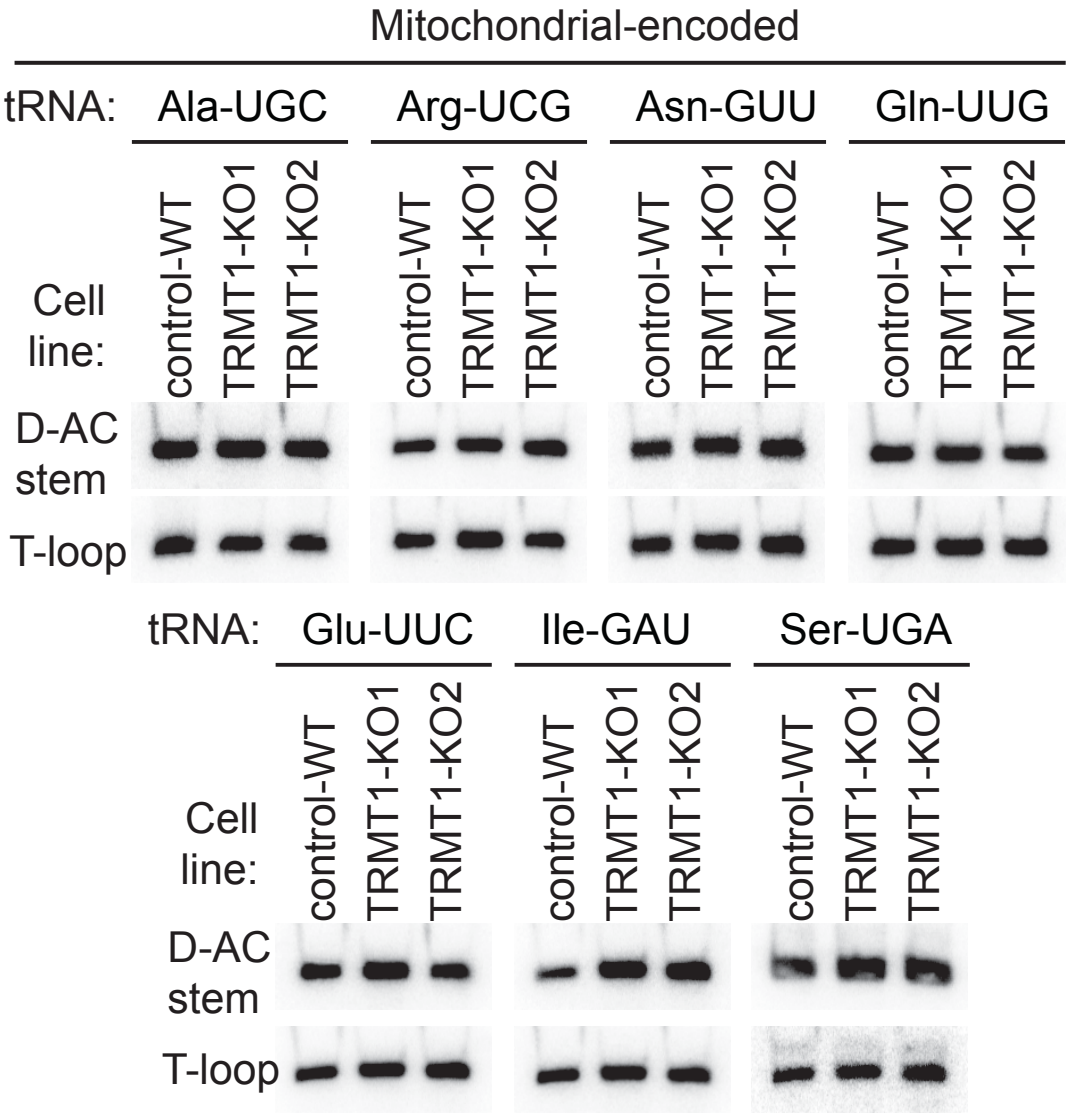

Supplemental Figure 3. *De novo* protein synthesis assays via puromycin labeling. (A) Nascent polypeptide chains labeled with puromycin from control-WT or TRMT1-KO cell lines were fractionated and detected by immunoblotting. Total protein serves as loading control. (B) Quantification of relative *de novo* protein synthesis as measured by the accumulation of puromycin-labeled polypeptides. The mean and standard deviation represents the puromycin signal of each cell line relative to control-WT after normalization to total protein from three independent labeling experiments. (C) Cells were incubated with the indicated concentration of puromycin in the absence or presence of cycloheximide (50 µg/mL) to block protein synthesis followed by harvesting and immunoblotting. (*) denotes a loading control protein that was probed simultaneously with the puromycin-labeled polypeptides.

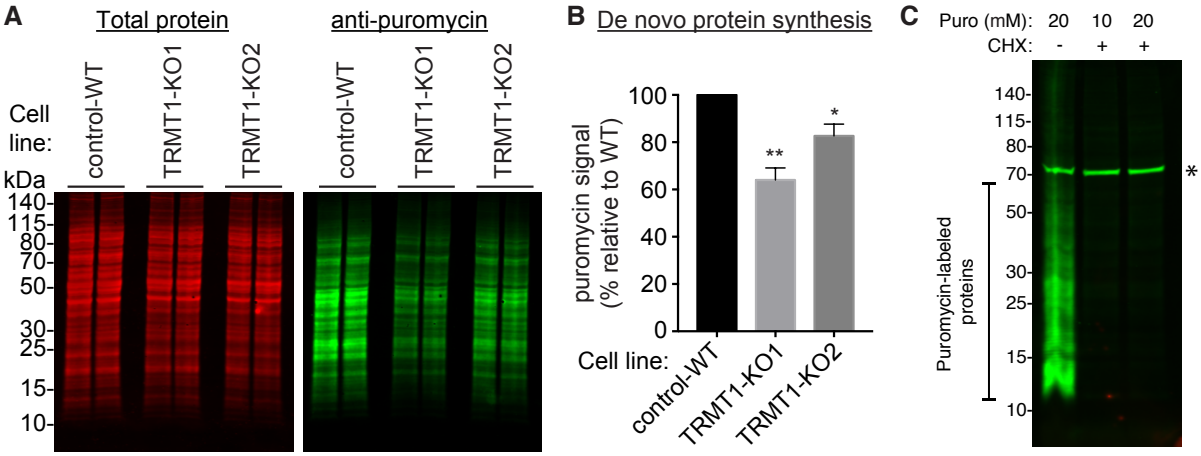

Supplemental Figure 4. TRMT1-KO cell lines exhibit defects in ROS homeostasis without major changes in mitochondrial membrane potential or mitochondrial ROS. (A) Flow cytometry scatter plots measuring mitochondrial potential using TMRE. The percentage of depolarized/dead, dead, depolarized/live and polarized/live cells (green quadrant) are denoted. As a control, cells were treated with FCCP to dissipate the mitochondrial membrane potential (lower panels). (B) Quantification of three independent mitochondrial membrane potential assays. Plotted are the live cells with polarized mitochondria (green quadrant of scatter plot). (C) Flow cytometry histogram plots of the indicated cell lines stained with the mitochondrial ROS detection stain, MitoSox Red with relative quantification shown in (D). (E) Flow cytometry histogram plots of the indicated cell lines stained with the cytoplasmic ROS detection stain, CellRox Orange with relative quantification shown in (F). Error bars for ROS measurements represent the standard deviation of three independent experiments. (*) $p < 0.05$; (**) $p < 0.01$.

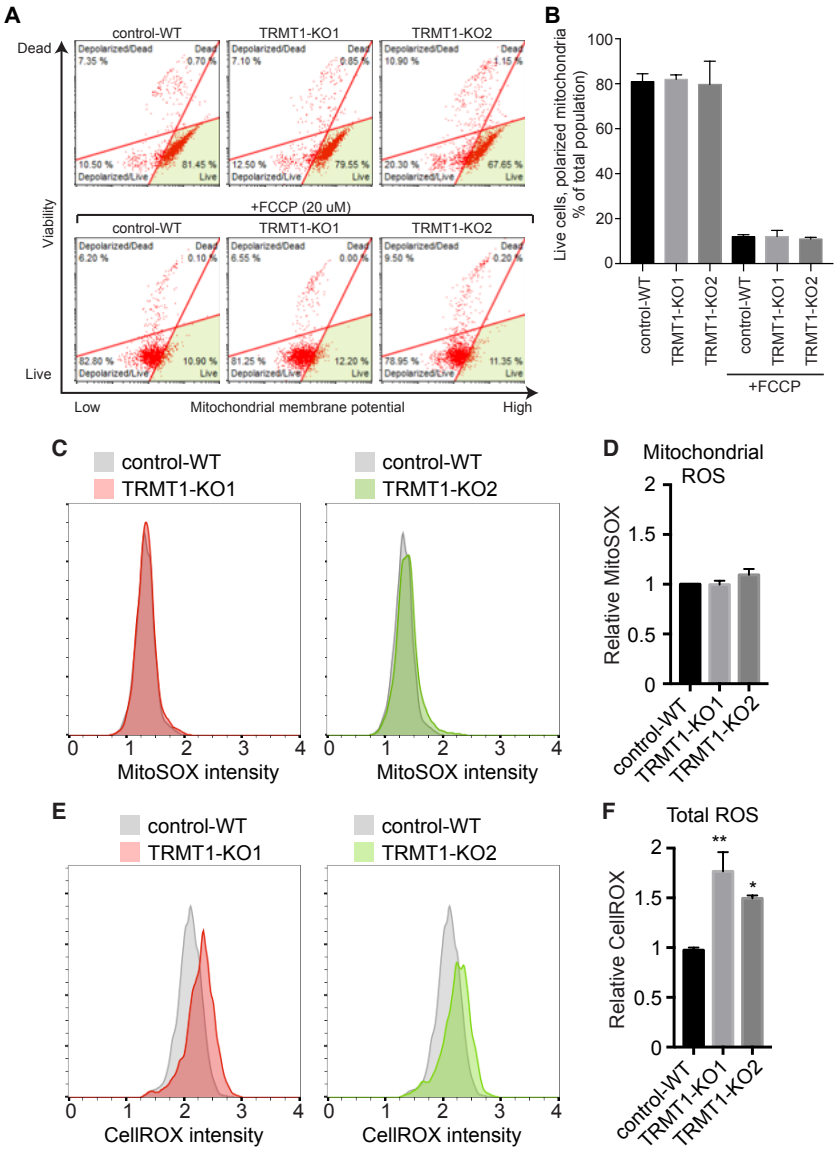

Supplemental Figure 5. Analysis of TRMT1 function in oxidative stress survival. (A, B) Flow cytometry scatter plots of propidium iodide-positive (dead cells) versus nucleated (total) cells after mock treatment (A) or exposure to *t*-bu-OOH (B). (C) The indicated cell lines were transfected with either empty vector or TRMT1 expression constructs followed by splitting into 6-well plates at 24-hours post-transfection. At 48-hours post-transfection, cells from one well of each transfection was harvested for extract preparation and immunoblot analysis while other wells were treated with *t*-buOOH (see Fig. 6). Error bars for (A) represent the standard deviation of three independent experiments. (**) $p < 0.01$; (***) $p < 0.001$; (****) $p < 0.0001$.

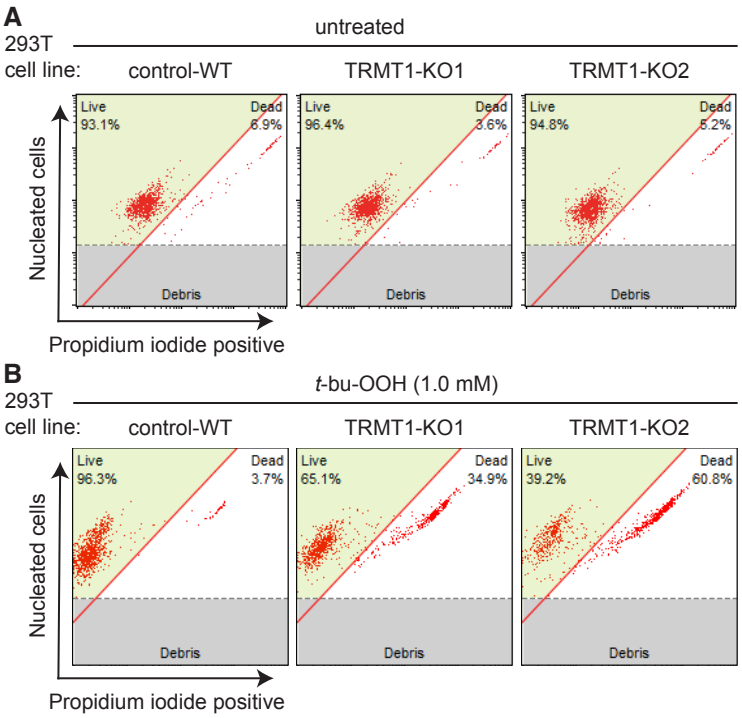

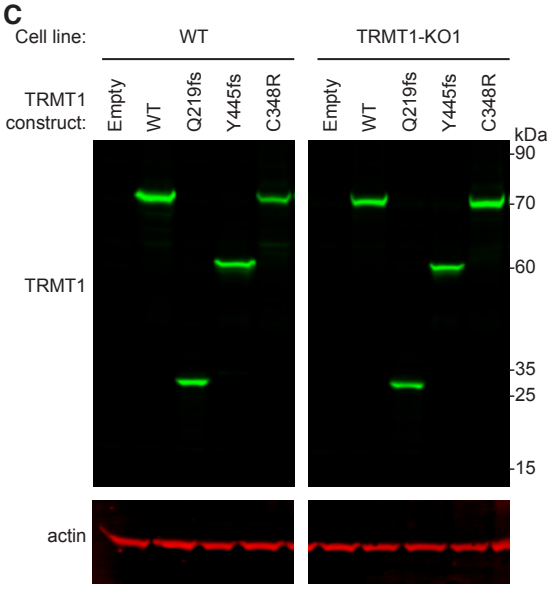

Table S1. Oligonucleotides used in this study.

TRMT1 cloning	**Sequence (5′-3′)**
TRMT1_HindIII_F	GAACT AAGCTT ATGCAAGGATCGTCTCTGTGGCTAA
TRMT1_NotI_R	CATGA GCGGCCGC TCAGTCTATGCCTGGCCCAGC
TRMT1_KpnI_F	GAACT GGTACC ATGCAAGGATCGTCTCTGTGGCTAA
TRMT1_NotI_R_nostop	CATGA GCGGCCGC GTCTATGCCTGGCCCAGCGG
TRMT1_ΔMTS_HindIII_F	GAACT AAGCTT ATGGAGAACGGCACCGGGCC
TRMT1_ΔMTS_KpnI_F	GAACTGGTACCATGGAGAACGGCACCGGGCC
silent_gs1_frag1_fwd	ccaagctggctagcgtttaaacttaagcttATGCAAGGATCGTCTCTG
silent_gs1_frag1_rev	aattcttggactggattgTAAAAGACCTCGTTGGCAC
silent_gs1_frag2_fwd	acgaggtcttttacaatccagtccaagAATTCAATCGGGACCTGACATG
silent_gs1_frag2_rev	ttaaacgggccctctagactcgagcggccgcTCAGTCTATGCCTGGCCC
C348R_frag1_fwd	ccaagctggctagcgtttaaacttaagcttATGCAAGGATCGTCTCTGTG
C348R_frag1_rev	ccgcagcccacacgCTGGAACACCAGCGCCTG
C348R_frag2_fwd	gctggtgttccagcGTGTGGGCTGCGGGGCCT
C348R_frag2_rev	ttaaacgggccctctagactcgagcggccgcTCAGTCTATGCCTGGCCCAGCG
TRTM1_ mut_F1(Q219)	gccagcgggagcccaagcttATGCAAGGATCGTCTCTG
TRTM1_ mut_R1(Q219)	cagatcgaTGGTACATCAGCATCCGG
TRTM1_ mut_F2(Q219)	gatgtaccaTCGATCTGGACCCCTATG
TRTM1_ mut_R2(Q219)	cctctagactcgagcggccgcTCAGTCTATGCCTGGCCC
Y445L_fs_frag1_fwd	caccctcagggccagcgggagcccaagcttATGCAAGGATCGTCTCTGTGGC
Y445L_fs_frag1_rev	tccagggtgtagtAGAGGCACGTCCGGGAGC
Y445L_fs_frag2_fwd	cggacgtgcctctACTACACCCTGGACCAGC
Y445L_fs_frag2_rev	ttaaacgggccctctagactcgagcggccgcTCAGTCTATGCCTGGCCC
CRISPR mutagenesis	
TRMT1 gs F1	CACCGGGTCTTTTATAACCCGGTGC
TRMT1 gs R1	AAACGCACCGGGTTATAAAAGACCC
TRMT1 gs F3	CACCGCGTGGACGTTCTTCTCCGTA
TRMT1 gs R3	AAACTACGGAGAAGAACGTCCACGC
TRMT1-gPCR-HIII-F2	GAACT AAGCTT agtcatccccaaaacgaggg
TRMT1-gPCR-BHI-R6	CGC GGATCC cccaggcagggagataaactt
T-loop (nuclear encoded tRNAs)	
Ala-AGC-G57	TGGAGAATGYGGGCGTCGATCCC
Arg-ACG-G59	GAGCCAGCCAGGAGTCGAACCT
Asn-GTT-G56	CGCTaACCGATTGCGCCACAGAGAC
Gly-CCC	TGATACCACTACACCAGCGGCGC
Leu-CAA	TGTCAGAAGTGGGATTCGAACCCACGC
Met-CAT	AACTCACGACCTTCAGATTATG
Phe-GAA	GGGATCGAACCAGGGACCTTTAGATC
Ser-AGA	GCGCGGGGAGACCCCAATGGATT
Thr-CGT	AGGCACGGACGGGGTTCGAACC
Trp-CCA	CCCCGACGTGATTTGAACACGCAa
Val-CAC	GGaCCTTTCGCGTGTGAGGCGA
Ile-TAT 5′-exon	TAT AAG TAC CGC GCG CTA AC
D-AC probes (nuclear encoded tRNAs)	
Ala-AGC-G57	TGCTAAGCACGCGCTCTACCACT
Arg-ACG-G59	TCCGTAGTCAGACGCGTTaTCCAT
Asn-GTT-G56	ACAGCCGAACGCGCTaACC
Gly-CCC	AATGGGAATCTTGCATGATACCACT
Leu-CAA	CTTGAGTCTGGCGCCTTAGAC
Met-CAT	GAGACTGACGCGCTGCCTACT
Phe-GAA	TCTTCAGTCTAACGCTCTCCCAAC
Ser-AGA	ATTTCTAGTCCATCGCCTTaACCAC

Thr-CGT	AGACCGACGCCTTACCACTT
Trp-CCA	TCTGGAGTCAGACGCGCTACCG
Val-CAC	TGTGAGGCGAACGTGATaACCACT
IleTAT 3'exon	CGAACTCACAACCTCGGCAT
T-loop probe (mitochondrial-encoded tRNAs)	
Ala-TGC	ACTCTGCATCAACTGAACGCAAATCA
Arg-TCG	TAAATATGATTATCATAATTTAATGAGTCGAAATC
Asn-GTT	CCCTAATCAACTGGCTTCAATCTA
Gln	GCCACCTATCACACCCCATCCTA
Glu	TCGCACGGACTACAACCACGA
Ile-GAT	GGGTTTAAGCTCCTATTATTTACTCTATCAAA
Ser-TGA	CAAAAAAGGAAGGAATCGAACCCC
D-AC probe (mitochondrial encoded)	
Ala-TGC	GAACGCAAATCAGCCACTTTAATTAA
Arg-TCG	GAGTCGAAATCATTCGTTTTGTTTAAA
Asn-GTT	GTTAACAGCTAAGCACCCTAATCA
Gln	ATCCAAAATTCTCCGTGCCACCTAT
Glu	ATATGAAAAACCATCGTTGTATTTCAACT
Ile-GAT	TCTATCAAAGTAACTCTTTTATCAGAC
Ser-TGA	AAGCCAACCCCATGGCCTCC
Primer extension	
IleTAT 55-34	AACTCACAaCCTCGGCATTATA
AlaAGC 54-36	TCCCGCTACCTCTCGCATG
Met-CAU_55-34	AACTCACGACCTTCAGATTATG
Phe-GAA_63-37	CGGGATCGAACCAGGGACCTTTAGATC
Ile-GAU mito 54-30	TTAAGCTCCTATTATTTACTCTATC
Additional Northern blot probes	
tRNA-Glu-UUC	CCAGGAATCCTAACCGCTAGACCATRTGGGA
U6 snRNA	CGTTCCAATTTTAGTATATGTGCTGCCGAAGCGA

Table S2. Mass spectrometer parameters of all analyzed nucleosides

Compound Name	Precursor Ion	Product Ion	Ret Time (min)	Delta Ret Time	Fragmentor Voltage	Collision Energy (eV)	Cell Accelerator Voltage	Polarity
15N dA (internal standard)	257	141	7,3	2	380	10	2	Positive
ac4C	286	154	6,8	2	380	10	2	Positive
Am	282	136	8,8	2	380	10	2	Positive
Cm	258	112	4,4	2	380	10	2	Positive
cm5U	303	171	1,9	1	380	10	2	Positive
cm5Um	317	171	4,4	2	380	10	2	Positive
D	247	115	1,7	1	380	10	2	Positive
Gm	298	152	6,5	2	380	10	2	Positive
I	269	137	4,7	2	380	10	2	Positive
i6A	336	204	14,2	2	380	10	2	Positive
m1A	282	150	2,8	2	380	10	2	Positive
m1G	298	166	6,4	0,5	380	10	2	Positive
m2,2G	312	180	8,1	2	380	10	2	Positive
m2G	298	166	6,8	0,5	380	10	2	Positive
m3C	258	126	3,3	1	380	10	2	Positive
m3U	259	127	5,9	1	380	10	2	Positive
m5C	258	126	4	1	380	10	2	Positive
m5s2U	275	143	7,5	2	380	10	2	Positive
m5U	259	127	5,1	1	380	10	2	Positive
m62A	296	164	12,5	2	380	10	2	Positive
m6t6A	427	295	10	2	380	10	2	Positive
m7G	298	166	4	2	380	10	2	Positive
mcm5U	317	185	6,5	2	380	10	2	Positive
mcm5Um	331	153	8,9	2	380	10	2	Positive
ms2i6A	382	250	16	2	380	10	2	Positive
Psi	245	191	1,7	2	380	10	2	Positive
Q	410	295	5,7	2	380	10	2	Positive
t6A	413	281	8,4	2	380	10	2	Positive
Um	259	113	5,7	2	380	10	2	Positive